

# Supporting Information

## 1 The influence of alkali metal cations upon AQ redox system

Figure 1 depicts the anthraquinone-2-sulfonate (AQ) redox signals in aqueous solutions supported with various alkali metal cations (ionic strength = 0.1 M) on a macro-Au electrode. Upon increasing the electrolyte cation sizes from sodium to rubidium (less commonly used as the supporting electrolyte/buffer cation), the voltammetric signals demonstrate no significant differences in the resulted AQ redox waves in aqueous solutions. This likely suggests that the alkali metal cations have insignificant degree of ion-pairing with neither the parent nor the reduced AQ species. Consequently a single  $2e^-$  reduction wave is obtained. The formal potential of the reaction,  $E_f^{\text{RXN}}$ ,  $(E_1+E_2)/2$ , occurs  $-0.62 \pm 0.005$  V ( $20 \pm 2$  °C) for all three reaction systems.

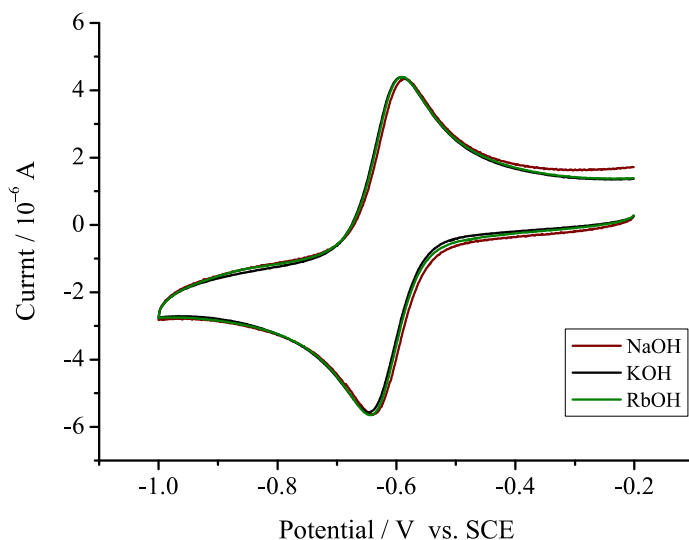
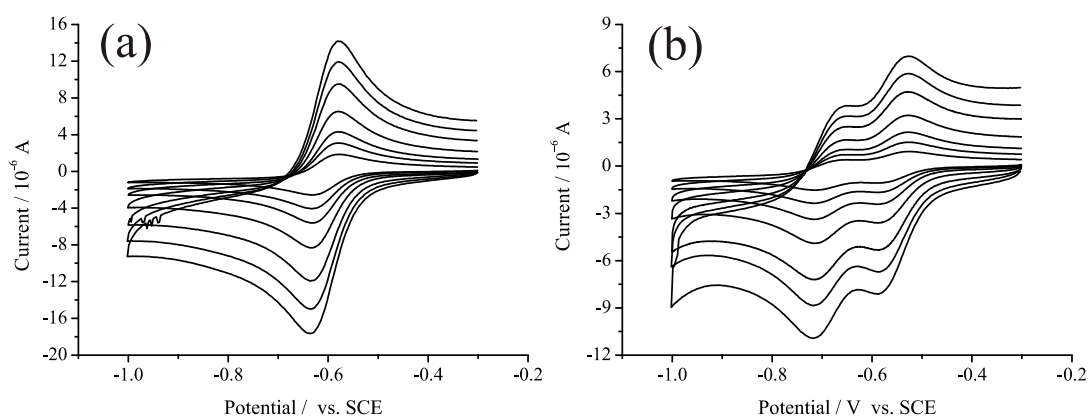


Figure 1 Cyclic voltammograms of 500  $\mu\text{M}$  AQ/  $\text{H}_2\text{O}$  supported with various alkali metal cations of increasing size from  $\text{Na}^+$ ,  $\text{K}^+$  to  $\text{Rb}^+$  at  $100 \text{ mV s}^{-1}$  on a macro-Au electrode.

## 2 Characterization of the AQ redox signals

The voltammetric signals of the AQ redox centre can be characterized via variation of scan rate over a range of 20-800  $\text{mV s}^{-1}$  on a macro-Au electrode. Figure 2 depicts the AQ voltammetric responses in aqueous solutions supported with 0.1 M tetramethylammonium hydroxide (TMAOH, a) and tetra-n-butylammonium (TBAOH, b), respectively. It is obvious to see that the formal potentials of the first and second electron transfers are independent with scan rate variation. This is characteristic of an EE reaction.<sup>1</sup>



**Figure 2** Cyclic voltammograms of AQ redox signals in aqueous solutions supported with 0.1 M (a) TMAOH, and (b) TBAOH electrolyte at  $100 \text{ mV s}^{-1}$  on a macro-Au electrode.

In addition, the reductive peak current was plotted against the square root of scan rate for the TMAOH supported reaction solution system. As shown in Fig. 3, a linear relationship was obtained ( $R^2=0.9997$ ). From the Randles-Ševčík equation, eqn (1), for a reversible  $n$  electron diffusional process, it was possible to obtain an *apparent* diffusion coefficient,  $D_o$ , from the gradient of the line.<sup>2</sup>

$$i_p = (2.69 \times 10^5) n^{1.5} A C_o D_o^{0.5} v^{0.5} \quad (1)$$

Here,  $i_p$  is the peak current (A),  $n$  is the total number of electrons transferred,  $A$  is the electrode area ( $\text{cm}^2$ ),  $C_o$  is the bulk concentration of the analyte ( $\text{mol cm}^{-3}$ ),  $D_o$  is the diffusion coefficient ( $\text{cm}^2 \text{s}^{-1}$ ), and  $v$  is the scan rate ( $\text{V s}^{-1}$ ). The gradient obtained was  $1.676 \times 10^{-5} \text{ A (V s}^{-1}\text{)}^{-0.5}$ , and consequently the *apparent*  $D_o$  was calculated as  $4.8 \times 10^{-6} \text{ cm}^2 \text{ s}^{-1}$ . This value is in contrast to the one obtained via a micro-Au electrode ( $5.3 \times 10^{-6} \text{ cm}^2 \text{ s}^{-1}$ ), as shown later in section 3. The underestimation caused by applying Randles-Ševčík equation is due to the assumption of concerted two-electron transfers, i.e. the second electron transfer is sufficiently driven. Nevertheless, consecutive electron transfer steps are commonly encountered for organic molecules where the second electron transfer is insufficiently driven.<sup>3</sup>

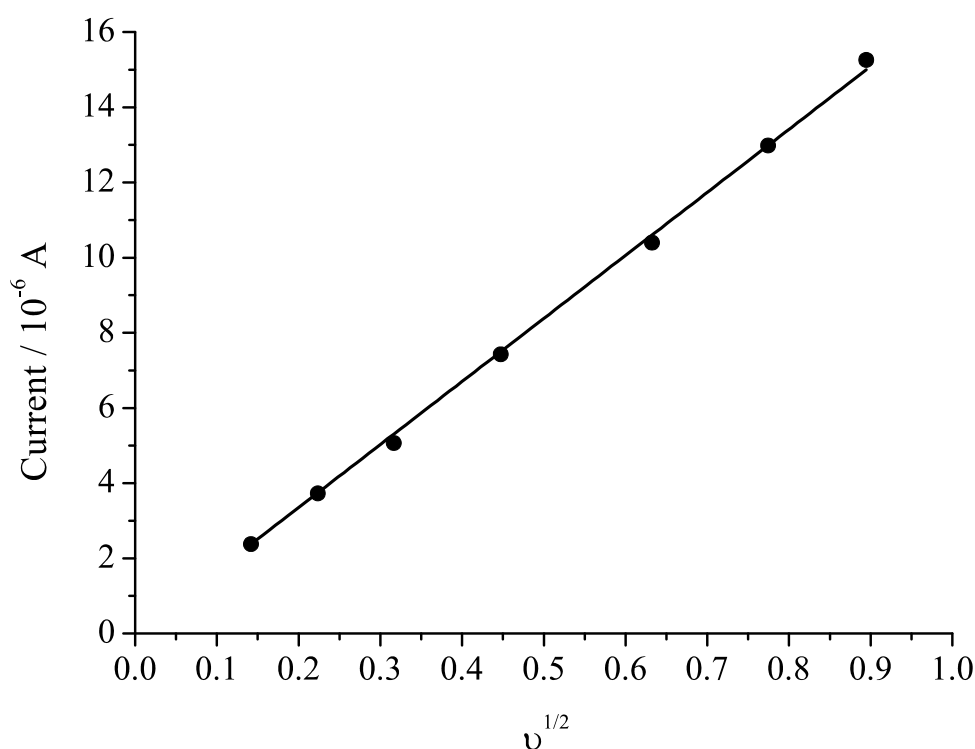


Figure 3 Plot of reductive peak current against square root of scan rate for 500  $\mu\text{M}$  AQ/  $\text{H}_2\text{O}$  supported with 0.1 M TMAOH electrolyte. The black line is the best fit through origin ( $R^2=0.9997$ ).

### 3 AQ redox system simulations

All simulations were performed by using the commercially available software package DIGISIM<sup>®</sup> (version 3.0, BASi Technical, USA). Digisim is based on a fully implicit finite difference (IFD) method as proposed by Rudolph.<sup>4,5</sup> A simple two-electron redox system (EE) was set up involving no protonation equilibrium due to high pH environment (above ~12) of the reaction solution.<sup>2</sup> All electron transfer rates were  $10 \text{ cm s}^{-1}$ , representing fast electron transfer processes. The transfer coefficient,  $\alpha$ , is 0.5 in all simulations, which assumes that the first electron transfer is the rate determining step.

In order to obtain the  $D_o$ s and fit them in simulations, they were experimentally measured in solutions supported by various sizes of electrolyte cations. A gold microdisc electrode was pre-calibrated first via chronoamperometry. The electrode was scanned at  $10 \text{ mV s}^{-1}$  in an acetonitrile solution containing 2 mM ferrocene and 0.1 M tetra-n-butylammonium perchlorate. The diffusion coefficient of ferrocene in acetonitrile is known to be  $2.3 \times 10^{-5} \text{ cm}^2 \text{ s}^{-1}$ ,<sup>1</sup> the electrode radius was accurately determined by fitting the obtained chronoamperomogram with Shoup and Szobo equation.<sup>6</sup>

Then the calibrated electrode was scanned by using cyclic voltammetry at  $10 \text{ mV s}^{-1}$  in a  $500 \mu\text{M}$  AQ aqueous solution supported by 0.1 M hydroxide salt with various electrolyte cation sizes. A steady-state current,  $i_{ss}$ , at a microdisc electrode was obtained, described in equation (2).

$$i_{ss} = 4nFD_oC_o r_o \quad (2)$$

where  $n$  is the number of electrons transferred per molecule diffusing to the electrode surface,  $F$  is the Faraday constant,  $D_o$  is the diffusion coefficient,  $r_o$  is the electrode radius, and  $C_o$  is the bulk concentration of redox active reagent.<sup>1</sup> The experimentally obtained  $i_{ss}$  and their corresponding  $D_o$ s are recorded in Table 1.

**Table 1. Experimentally obtained diffusion coefficients via steady-state currents.**

Electrolyte (I=0.1M)	100% TBAOH	(60+40)% TBAOH +TMAOH	(20+80)% TBAOH +TMAOH	100% TMAOH	100% KOH
$i_{ss} / \text{nA}$	1.62	1.89	2.22	2.86	3.05
$D_o / \times 10^{-6} \text{ cm}^2 \text{ s}^{-1}$	3.0	3.5	4.1	5.3	5.65

The diffusion coefficients ( $D_o$ ) were set as same value for both the parent and reduced quinone species in each reaction solution system. In reality, the solvation sphere is different for unequally charged anions. However it is a fair assumption, which can be confirmed by the excellent fitting of the simulated and the experimental results. The simulation has discarded the comproportionation mechanism, which is proposed<sup>7</sup> to be blind only if the  $D_o$ s are equal and electron transfer rates are fast.

The simulated voltammograms are aimed to match with the experimental peak currents, peak potentials and wave shapes. Figure 4 shows the overlaid simulated and experimental results for AQ (500  $\mu\text{M}$ ) redox reaction in aqueous solutions supported by four different supporting electrolytes. The excellent fittings, therefore, enable us to obtain the formal potentials of the first and second electron transfers in the AQ reduction process.

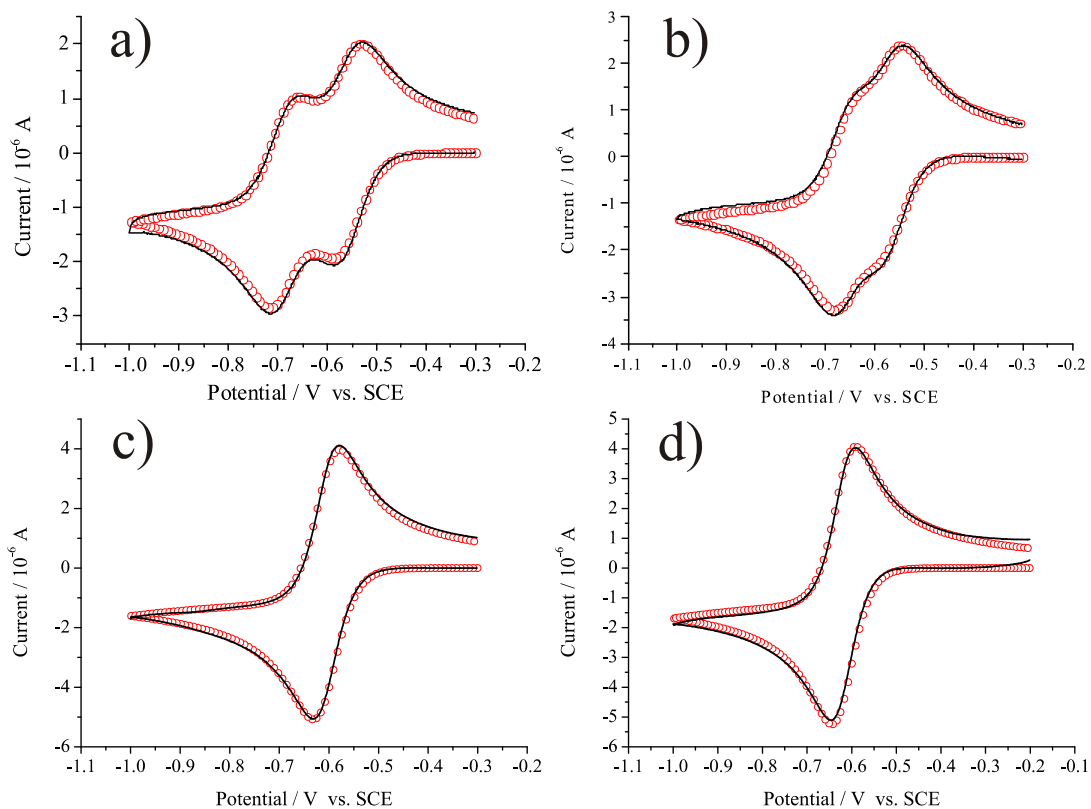


**Figure 4** Overlaid experimental (black line) and simulated (red circles) cyclic voltammograms of 500  $\mu\text{M}$  AQ redox signals in aqueous solutions at  $100 \text{ mV s}^{-1}$  supported with various supporting electrolyte (ionic strength= 0.1 M) cations: a) TBAOH, b) 60%TBAOH + 40%TMAOH, c) TMAOH and d) KOH.

## 4 The existing forms of oxygen intermediate species in the oxygen reduction reaction

At pH above 12, the superoxide radical species is present in its un-protonated form due to low  $pK_a$  of the couple  $HO_2^\bullet$  and  $O_2^{\bullet-}$  being 4.88.<sup>8</sup> The  $pK_{a1}$  value of  $H_2O_2$  is 11.62,<sup>8</sup> and the second acid dissociation constant ( $pK_{a2}$  of  $HO_2^{\bullet-}$ ) is expected to be even larger. This means that, in 0.1 M hydroxide aqueous solution ( $pK_a$  of  $H_2O = 15.7$ ) the peroxide anion is most likely present in its mono-protonated form.

## References

1. A. J. Bard and L. R. Faulkner, *Electrochemical Methods: Fundamentals and Applications*, Wiley, New York, 2nd Edn, 2001.
2. C. Batchelor-McAuley, Q. Li, S. M. Dapin and R. G. Compton, *J. Phys. Chem. B*, 2010, **114**, 4094.
3. Q. Li, C. Batchelor-McAuley and R. G. Compton, *J. Phys. Chem. B*, 2010, **114**, 7423.
4. M. Rudolph, *J. Electroanal. Chem.*, 1991, **314**, 13.
5. M. Rudolph, *J. Electroanal. Chem.*, 1992, **338**, 85.
6. D. Shoup and A. Szabo, *J. Electroanal. Chem.*, 1982, **140**, 237.
7. C. P. Andrieux and J. M. Savéant, *J. Electroanal. Chem.*, 1970, **28**, 339.
8. W. H. Koppenol, D. M. Stanbury and P. L. Bounds, *Free Radical Bio. Med.*, 2010, **49**, 317.